HHS Public Access

Author manuscript

Nat Ecol Evol. Author manuscript; available in PMC 2017 November 15.

Published in final edited form as:

Nat Ecol Evol. ; 1(6): 152. doi:10.1038/s41559-017-0152.

Perceptive Costs of Reproduction Drive Aging and Physiology in Male *Drosophila*

Zachary M. Harvanek[1,2], **Yang Lyu**[1], **Christi M. Gendron**[1], **Jacob C. Johnson**[1], **Shu Kondo**[3], **Daniel E. L. Promislow**[4,5], and **Scott D. Pletcher**[1,6,*]

[1]Department of Molecular & Integrative Physiology, University of Michigan, Ann Arbor, 48109

[2]Medical Scientist Training Program, University of Michigan, Ann Arbor, 48109

[3]Genetic Strains Research Center, National Institute of Genetics, Mishima, Shizuoka, Japan

[4]Department of Pathology, University of Washington, Seattle, WA 98195

[5]Department of Biology, University of Washington, Seattle, WA 98195

[6]Geriatrics Center, University of Michigan, Ann Arbor, 48109

Abstract

Costs of reproduction are thought to result from natural selection optimizing organismal fitness within putative physiological constraints. Phenotypic and population genetic studies of reproductive costs are plentiful across taxa, but an understanding of their mechanistic basis would provide important insight into the diversity in life history traits, including reproductive effort and aging. Here we dissect the causes and consequences of specific costs of reproduction in male *Drosophila melanogaster*. We find that key survival and physiological costs of reproduction arise from perception of the opposite sex, and they are reversed by the act of mating. In the absence of pheromone perception, males are free from reproductive costs on longevity, stress resistance, and fat storage. Both the costs of perception and the benefits of mating are mediated by evolutionarily conserved neuropeptidergic signaling molecules, as well as the transcription factor *dFoxo*. These results provide a molecular framework in which certain costs of reproduction arise as a result of self-imposed 'decisions' in response to perceptive neural circuits, which then orchestrate the control of life-history traits independent of physical or energetic effects associated with mating itself.

*Corresponding Author.

CONTRIBUTIONS

Z.M.H. and S.D.P. conceptualized the project, and Z.M.H., Y.L., D.E.L.P., and S.D.P. designed the experiments. Z.M.H., C.M.G., and J.C.J. performed the *in vivo* experiments, and Z.M.H., C.M.G., and S.D.P. analyzed them. D.E.L.P. performed the metabolomics. Y.L. and S.D.P. analyzed the metabolomics data, with input from Z.M.H. and D.E.L.P. S.K. created the NPF mutant used in figure 3. Z.M.H., Y.L., and S.D.P. wrote the manuscript, with comments from C.M.G. and D.E.L.P.

COMPETING INTERESTS

The authors declare no competing financial interests in this publication.

INTRODUCTION

Costs of reproduction represent a set of putative fitness trade-offs through which enhanced reproductive effort compromises future survival and limits lifespan. Putative costs of reproduction have been characterized as either ecological or physiological in nature[1], and they have been described in nearly all taxa, from brine shrimp[2], nematodes[3] and fruit flies[4] to rodents[5] and primates[6], including humans[7,8]. Ecological costs of reproduction represent environmental dangers that result from reproductive behavior, including increased risk of predation and disease. As such, their causes and consequences are often identifiable and best studied in natural conditions[9]. In human societies, and in laboratory settings, ecological costs of reproduction are reduced or largely eliminated.

Physiological costs of reproduction manifest because limited resources necessitate that most biological functions receive allotments that are inadequate to sustain their long-term function, leading to a reduction in future health and survival. They may result from physical constraints that limit an organism's food intake, which imposes a ceiling on its energetic output. They also involve physiological decisions through which a finite amount of available energy is partitioned between reproduction and survival such that neither is at its theoretical maximum[10]. Physiological costs of reproduction have been described at the phenotypic and population genetic levels in a wide range of species, and they are generally recognized as the most significant components underlying life-history trade-offs[9]. The biological mechanisms underlying these costs, however, have been decidedly more difficult to identify[1,10–12].

Mechanistic insights about costs of reproduction have come largely from experiments using the fruit fly, *Drosophila melanogaster*[4,13–17], and reviewed in[12]. These experiments have examined costs in both males and females, and surprisingly, they have failed to implicate physiological or energetic trade-offs. Even studies in which a connection to energetics has been shown through dietary restriction[18] or by measuring energy stores[19] conclude there is no simple trade-off between reproduction and somatic investment. In female flies, costs of reproduction arise in part from the transfer of the seminal fluid protein Sex Peptide from males to females during mating, which increased female mortality rates and decreased lifetime reproductive output. This occurred despite an increase in food intake[20] and decrease in mating frequency[16], both of which should result in a net increase in energy availability. In males, the molecular mechanisms underlying reproductive costs are a mystery. One study demonstrated that male flies exposed to cauterized females, which do not mate, suffered from decreased lifespan beyond those of males exposed to normal females, revealing a cost of reproduction that manifests in the absence of mating itself[17]. The authors suggested increased energy expended by courtship as the cause for this effect, but this seems unlikely as recent studies have shown that activity in general and exercise in particular are not sufficient to affect lifespan[21].

In this article, we dissect the mechanisms underlying the costs of reproduction on both longevity and specific markers of health in male *Drosophila*. We show that changes in survival and key physiological costs occur in response to the animal's perceived reproductive environment, independent of any physical or energetic effects associated with mating itself. We also find that mating *promotes* health and lifespan in this context by

reversing the phenotypic consequences of perception and that this phenomenon is potentiated by the neuropeptide Corazonin (*Crz*), which is the fly homolog of vertebrate gonadotropin-releasing hormone. In the absence of perception, male *Drosophila* experience no measurable survival costs of mating itself. Physiological changes in peripheral tissues that occur in response to pheromone perception require the activity of the transcription factor *dFoxo*, independent of systemic insulin signaling. Self-imposed biological responses to reproductive perception likely exist across taxa[22], and therefore may constitute an important mechanism underlying variation in life history strategies observed in nature.

RESULTS

Pheromone perception drives costs of reproduction and mating ameliorates them

Recent results from experiments using *Drosophila* and the nematode, *Caenorhabditis elegans*, suggested that costs of reproduction on lifespan may be biologically regulated responses to the perception of the opposite sex, rather than physical constraints or energetic limitations in reproductively active animals[22–24]. Male *Drosophila* that perceived female pheromones, but did not mate, showed decreased lifespan, triglyceride stores (a major storage form for lipids in flies), and stress resistance[23]. Similar effects of sexual perception were observed in hermaphrodite *C. elegans*, suggesting that this phenomenon may be evolutionarily conserved[22].

To explore the role of pheromone perception in costs of reproduction on health and longevity in male *Drosophila*, we manipulated the perceived sexual environment of experimental animals independently of their mating opportunities. To do this, we replaced the pheromone profile normally produced by a male or female fly with one characteristic of the opposite sex. Male flies that produced female pheromones (termed ‘feminized males’ and symbolized by ♂(♀)) were created by targeting expression of the sex determination gene, *tra*, to the oenocytes (via *OK72-GAL4*), whereas masculinization of female flies (♀(♂)) was accomplished by expressing *tra*-RNAi in a similar way[23]. These transformed animals, together with animals that produced pheromones consistent with their genetic sex (noted as ♂ (♂) and ♀(♀) for males and females, respectively), constituted four groups of “donor” animals that were independently housed with experimental males (Fig. 1A). To measure the physiological and lifespan effects of sexual perception without changes in reproductive opportunity, we compared experimental males housed with donor flies that were of the same sex (either male or female) but that expressed pheromone profiles characteristic of different sexes. Conversely, to measure the effects of reproduction without changes in pheromone perception, we compared experimental males that were housed with either male or female donor flies that expressed the same pheromone profiles (Fig. 1A).

We found that phenotypic effects on survival and metabolism were due to sexual perception. When we housed experimental males with feminized male donor animals (♂(♀)), thus precluding the possibility of mating, the presence of female pheromones significantly decreased starvation resistance, reduced total levels of stored triacylglyceride (TAG), and shortened lifespan compared with experimental males housed in the presence of male donors (♂(♀) vs. ♂ (♂), Fig. 1B–D, Fig. S1), as previously shown[23]. However, we failed to observe significant differences in these phenotypes when comparing experimental males that were

housed with masculinized female donor flies, which produced male pheromones, to those housed with male donor flies (♀(♂) vs. ♂ (♂)).

Our failure to observe measurable costs of reproduction on survival, fat storage, or stress resistance was not because males did not mate with masculinized females. In competitive environments, males only modestly preferred females with female pheromone profiles to those that had been masculinized (27/41 = 66% of the time, P = 0.06, binomial exact test). The majority of flies (31/41=76%) mated with both females, and males that first chose a ♀(♀) female were slower to remate than males that first chose a ♀(♂) female (Fig. S2A). Furthermore, in experimental conditions where males were exposed to only one type of female, we routinely observed similar numbers of fertilized eggs in cohorts exposed to ♀(♀) and ♀(♂) donor females, and mating latency (Fig. S2B) and fertilization rates (Fig. S2C) were not significantly different.

Exposure to female pheromones reduced TAG storage, stress resistance, and lifespan. However, when we compared the effects of female pheromones as presented by male (♂(♀)) or female (♀(♀)) donor animals, we found that the negative effects of female pheromone exposure were significantly ameliorated when experimental males were exposed to ♀(♀) females and thus allowed to mate (compare red to yellow groups in Fig. 1B–D, Fig. S1). This is unexpected, considering that costs of reproduction are thought to represent energetic requirements that include courtship and copulation.

To investigate whether aggressive or courtship behaviors were responsible for the phenotypic differences we observed, we collected video of freely behaving experimental flies in each of the four exposure conditions. We did not observe any appreciable frequency of aggression (e.g., male-male escalation) in any treatment, confirming results reported previously[23]. We also quantified reproductive interactions (i.e., courtship behaviors) in male flies housed in each of our four treatments. Males exposed to feminized males exhibited an equal reproductive investment (e.g., courtship time) with donor animals as did experimental males exposed to females, although these interactions were shorter on average (Figs S2D and S2E). Less time was devoted to masculinized females and control males. These results were supported by a wing-damage assay over a longer (14 day) time period where minor wing damage was more common in males exposed to female pheromones than male pheromones, independent of the donor animal's sex (Fig. S2F). We therefore conclude that survival differences among our four exposure treatments are not driven by different levels of aggression, and they do not correlate well with levels or intensity of courtship.

To further test the hypothesis that the male's perception of female pheromones is required for the costs of reproduction on health and longevity, we repeated our survival experiments using experimental males that carried a loss of function mutation in the pheromone receptor *ppk23*[25]. Unlike control males (Fig. S3A), *ppk23* mutant males showed no lifespan differences whether they were exposed to ♂ (♂) (no mating or pheromones), ♀(♂) (mating alone), or ♀(♀) (pheromones and mating) donor animals (Fig. 1E). *ppk23* mutant males were therefore long-lived in a mixed-sex environment when compared to wild-type males (Fig. S3B). In the absence of female pheromones, the *ppk23* mutation had no influence on lifespan (Fig. S3C). Loss of *ppk23* also prevented the cost of reproduction effects on

starvation resistance (Figs. S3D and S3E). In mixed-sex environments, reproductive output from *ppk23* males (as measured by the number of offspring sired per vial) was surprisingly higher than that of control males throughout life despite their extended lifespan (Fig. S4). One possible explanation is that mating with the *ppk23* mutant males is less harmful to females, allowing for increased reproductive output. Together, these data indicate that the lifespan extension in *ppk23* mutant males results from the elimination of perceptive costs of reproduction on survival and that reproduction itself is not costly.

Pheromones and mating have distinct effects on the neurometabolome

Because of the involvement of sensory circuits in the costs of reproduction on survival, we predicted that short-term effects of perception would influence the brain states of experimental males. We therefore compared metabolite abundances in heads of experimental males that had been exposed to ♂(♂), ♂(♀), or ♀(♀) donor animals for 48 hours. Untargeted metabolite analysis identified 524 and 409 metabolites present in all treatments for positive and negative modes, respectively (see supplementary information for raw data). Using a randomization procedure together with principal component analysis (PCA) we identified a single principal component (PC5) that significantly distinguished different treatments (Figs. 2A and 2B). Strikingly, this PC separated groups based only on pheromone exposure; the neurometabolome of male flies exposed to ♂(♀) (pheromones alone) essentially overlapped in this space with the neurometabolome of male flies exposed to ♀(♀) (pheromones and mating). Both were clearly distinct from that collected from males exposed to ♂(♂) donor animals. These results suggest that the neurological signature of reproductive activity is faithfully recapitulated by the mere perception of available females.

We next asked whether mating influenced the effects of perception on the neurometabolome. We therefore repeated the previous experiment with the addition of a fourth exposure treatment in which experimental males were exposed to masculinized females (♀(♂)). In this case, we identified two positive mode metabolome principal components (PC2 and PC3) that provided a statistically significant ability to resolve treatments (Fig. 2C). One principal component (in this case PC3) separated the neurometabolomes of experimental males according to pheromone perception, grouping ♂(♂) and ♀(♂) exposure treatments together and separating them from ♀(♀) and ♂(♀) exposures (Fig. 2D, Fig. S5A). PC2 separated the treatments according to mating status, grouping the female exposures apart from the male exposures (Fig. 2D, Fig. S5A). Both PC2 and PC3 provided significant separation of their respective phenotypes when compared to random permutations (Fig. S5A). Similar results were observed using the negative mode data (Fig S5B). PC2 and PC3 showed increased weighting of molecules that were differentially produced between either mating/non-mating groups or male/female pheromone groups, respectively, reinforcing the importance of these components (Fig. S5C). Because PC2 and PC3 are orthogonal, these data indicate that the impact of mating on the neurometabolome is distinct from that of pheromone perception, suggesting that mating does not strictly reverse the effects of perception but instead induces distinct changes that ameliorate its consequences.

The top 20 metabolites based on PC2 or PC3 loadings are listed in Supplementary Table 1 (see Supplementary File 1 for all metabolite data). Metabolites associated with pheromone

exposure were enriched in glycerophospholipid metabolism (P = 0.022, Fisher's exact test), which plays an important role in modulating neural activity. Metabolites associated with PC2, the mating axis, were not significantly enriched for any specific pathway.

The neuropeptides npf and corazonin mediate self-imposed costs of reproduction

Our neurometabolomic data suggested that mating and pheromone exposure have distinct effects on brain state, indicating that mating may act through parallel neural circuits to rescue the deleterious consequences of pheromone exposure. We therefore sought to identify distinct subsets of neurons that are required for the effects of pheromones or mating. *Drosophila* neuropeptide F is the homolog of vertebrate neuropeptide Y, and it has been implicated in feeding and reward behaviors[26,27]. Gendron et al. (2014) inhibited *npf*-expressing neurons by expressing a temperature-sensitive dynamin mutant *shibire* (shi^{ts1}) and found that this significantly reduced the effects of female pheromones on male stress resistance. We reproduced those findings and implicated NPF directly using an *npf* mutant allele. We found that *npf* is required for the full effect of female pheromones on male lifespan (Fig. 3A), establishing that it is a key neuropeptide involved in modulating the perceptive costs of reproduction on longevity.

In a candidate screen designed to reveal suppressors of pheromone effects, we found that neurons expressing the neuropeptide *Corazonin*, which is the fly homolog of vertebrate gonadotropin-releasing hormone, mediate the beneficial effects of mating. When we inhibited *crz*-expressing neurons in adult experimental males, mating no longer rescued the deleterious effects of pheromone perception on lifespan (Fig. 3B). When we activated *crz*-expressing neurons, on the other hand, mating completely reversed pheromone costs, such that mating and exposure to female flies had no effect on male lifespan (Fig. 3C and Fig. S6). Notably, activating *crz*-expressing neurons was not sufficient to increase lifespan in same-sex cohorts, suggesting that this peptide specifically mediates the effect of mating on lifespan (Fig. 3C).

The transcription factor, *dFoxo*, modulates the physiological effects of perceptive costs of reproduction

We next sought to identify signaling pathways in peripheral tissues that are responsible for the effects of pheromone perception. Based on gene expression studies of aging and pheromone effects in flies and *C. elegans*[22–24,28–30] we carried out a survey of candidate genes and interventions to identify those that mediate the effects of perceptive costs of reproduction on starvation resistance and TAG storage (Table S2). This work identified the transcription factor *dFoxo* as a regulator of these effects. Indeed, two distinct *dFoxo* mutant alleles were resistant to pheromone effects on starvation resistance and TAG abundance ($dFoxo^{\Delta 94}$[31], and $dFoxo^{w24}$[32]; Fig. 4A–4B and S7A–S7B, respectively), as were flies that were trans-heterozygous for the two alleles (Fig. S7C). Furthermore, the $dFoxo^{\Delta 94}$ mutation nearly eliminated the effect of pheromones on lifespan (Fig. 4C), and the $dFoxo^{w24}$ mutation significantly reduced it (Fig. S7D). Pheromone exposure also decreased the expression of the *dFoxo* target gene *4EBP/Thor*[28]; Fig. S7E), suggesting a reduction of dFOXO activity upon pheromone exposure.

In *Drosophila*, three of the eight insulin-like peptides (*dIlp2*, *dIlp*3, and *dIlp*5) are produced in specialized neurosecretory cells in the *pars intercerebralis* (PI), the fly analog of the vertebrate hypothalamus[33]. Previous studies have suggested that the PI, and particularly dIlp2, modulate lifespan in flies[34,35], likely by inactivating dFOXO. Surprisingly, pheromone exposure did not alter the abundance of circulating dILP2 in the hemolymph (Fig. 4D), and simultaneous loss of the three centrally produced insulin-like peptides did not prevent the effects of pheromone exposure on starvation resistance or lifespan (Fig. 4E, 4F). Moreover, manipulation of both TOR signaling and *sir2* gene function did not prevent the effects of pheromone perception on lifespan (Fig. S8), suggesting that the effect of pheromone exposure on aging does not require other *dFoxo*-related aging pathways.

DISCUSSION

Costs of reproduction in male *Drosophila melanogaster* have been reported to compromise health and limit lifespan[12]. By taking advantage of genetic reagents that allowed us to manipulate mating opportunities independent of the social environment, we were able to investigate the mechanisms underlying these costs. In the absence of female pheromones or the ability to perceive them, reproductive behaviors, and in particular mating itself, have no negative effects on several major life history traits in males, including stress resistance, fat storage, and lifespan. Surprisingly, the act of mating itself was found to be beneficial when males perceived pheromones. These reproductive costs are, therefore, not inevitable but instead are self-imposed and regulated responses induced by the expectation of mating and caused by perception of the opposite sex.

Further dissection of the molecular connections among pheromone perception, mating, and physiologic costs in *Drosophila* would illuminate how reproduction and social interactions regulate the aging process. Global metabolomic profiling revealed that pheromone perception and mating cause discrete neurometabolomic ‘states’, as defined by characteristic abundances of metabolites. Distinct neural circuits likely mediate their effects, with *npf* required for the negative effects of pheromone perception and *crz*-expressing neurons modulating the beneficial effects of mating. It remains unknown how perceptive signals from *ppk23*-expressing neurons reach *npf*-expressing neurons, as the two populations do not appear to be directly connected[36,37]. Similarly, determining whether and how neuronal NPF and CRZ signaling influences dFOXO activity in peripheral tissues would provide important insight into the cell non-autonomous nature of reproductive physiology. Surprisingly, several pathways that interact with FOXO to modulate aging (dILPs 2, 3, and 5, along with TOR and sirtuin signaling) are dispensable for pheromonal effects on lifespan, suggesting the possibility of undiscovered regulatory mechanisms.

Several lines of evidence suggest that the signaling processes that we describe may influence costs of reproduction in female flies and in individuals of other species. Mating reversed observed costs of courtship that female *Drosophila* may have experienced upon exposure to males, and once the deleterious effects of sex peptide were removed, females were largely free of mating costs[16,38]. Furthermore, the influential pathways that we characterized in male *Drosophila* are evolutionarily conserved. The vertebrate homolog of corazonin is gonadotropin-releasing hormone (GnRH), which is known to regulate sexual behavior in

addition to reproductive physiology. GnRH-producing neurons are anatomically altered by social interactions in Cichlid fish[39], and GnRH itself has been linked to mammalian aging[40]. Notably, NPY, the vertebrate homolog of *npf*, interacts with GnRH neurons in mammalian systems[41,42]. These results suggest the NPY-GnRH axis deserves attention as a mechanism that might influence healthy aging in humans and could account in part for variation in life-history strategies across species in nature.

The notion that some, if not all, costs associated with reproductive effort result from the balance between decisions in response to reproductive expectation and the outcome or reward of those actions provides new context to existing literature and suggests new avenues for future research. Previous work demonstrated that males exposed to cauterized females live shorter than males exposed to control females. This finding was interpreted to be a result of energy expenditure of courtship and was termed a "cost of courtship"[17]. In light of our findings, these results might now be interpreted as due to pheromone exposure, with males exposed to non-cauterized females having the negative effects of pheromone exposure partially rescued by the beneficial effects of mating. In this view, costs of courtship result not from courting itself but instead from *the drive* to court, and the magnitude of the cost is influenced by whether male flies achieve reproductive success. This perspective may invoke reflections on human emotions, including frustration and desire, which may share mechanistic building blocks, or "emotion primitives," that are conserved across species[43]. In humans, psychological factors, such as perceived quality of life, have been linked to protective effects on mental health in advanced age[44], and copulation has been associated with a variety of health benefits[45,46]. Thus, future research on reproductive costs and aging may benefit from a focus on central neurological states and their influence on life-history traits through orchestrated physiologic responses in peripheral tissues.

METHODS

General fly husbandry

All flies used in this paper (including experimental and donor animals) were raised using the same methods. Eggs were collected from yeasted grape juice agar plates, and 32 μl of eggs were placed onto bottles containing a modified Caltech Medium (CT), a commonly used cornmeal-based food[47]. Unless otherwise noted (e.g., for neuronal activation/inhibition experiments), all flies were kept in a controlled humidity incubator at 25 °C in 12 hour light/dark conditions. Flies were collected into bottles containing 10% yeast/sucrose food within 24 hours of emergence, and (unless specified as virgin) were allowed to mate for 2–3 days, after which the flies were sexed into groups of 25 in vials containing 10% yeast/sucrose food. Flies were maintained on 10% yeast/sucrose food for the remainder of their life, with the exception of the candidate survey, during which flies were placed on 30% sucrose/5% yeast food for four days prior to sacrificing them for physiologic assays.

Fly stocks

The standard laboratory stocks *yw*, w^{1118}, and *Canton-S* were originally obtained from the Bloomington Stock Center. The *OK72-Gal4* line, *UAS-kir2.1* line, *UAS-Gal80*^{ts} line, and *Sir2* mutant lines were also obtained from the Bloomington Stock Center. *UAS-TRA* and

UAS-TRA^{DSRNA} were provided by B.J. Dickson. The *ppk23* mutant line was provided by K. Scott. The *npf* mutant line was created as described below. The *Crz-Gal4* line was provided by E. Johnson. Thus *UAS-TrpA1* line was provided by P. Garrity. The *dFoxo* and *dILP* mutant lines were provided by L. Partridge. The tagged-*dILP2* line was provided by S. Kim. The *AkhR* mutants and revertant controls were provided by R. Kühnlein. All lines except those used solely in the downstream effector screen (Table S2) were backcrossed at least 8 generations. *dFoxo* mutants were backcrossed following the effector screen, and all data not appearing within the table (i.e., in Figure 4 and Figure S7) were obtained using backcrossed lines.

npf mutant creation

NPF mutants were created by the transgenic CRISPR/Cas9 technique as previously described[48]. The gene-specific 20-bp sequence of the gRNA was GCCCTTGCCCTCCTAGCCGC. The deletion is an 11 base pair deletion near the 3′ end of the coding region and is as shown below:

WT
GGTTGCCTGTGTGGCCCTTGCCCTCCTAGCCGC**CGG**CTGCCGAGTGGAGG
CGTCCAACTC

SK2 GGTTGCCTGTGTGGCCCTTGCCCTCCT----------
GCCGAGTGGAGGCGTCCAACTC

Production of donor flies

Male donor flies were produced by crossing either *w*^{1118}*;UAS-TRA*;+ virgin females or *yw;UAS-TRA*;+ virgin females to either *w*^{1118}*;OK72-Gal4*;+ males (to create ♂$^{(♀)}$ donor flies) or to *w*^{1118};+;+ genetic controls (to create ♂$^{(♂)}$donor flies). Female donor flies were produced similarly, except *w*^{1118}*;+;UAS-TRA*^{DSRNA} virgin females were crossed to *w*^{1118}*;OK72-Gal4*;+ males to generate ♀$^{(♂)}$ donor flies and to *w*^{1118};+;+ genetic controls to create ♀$^{(♀)}$ donor flies.

Exposure to donor flies

Experimental flies were exposed to donor animals in a ratio of 5 experimental flies to 25 donor flies, unless otherwise stated (see also[23]). For physiologic and stress resistance assays, exposure began on day 8–10 after eclosion, except when performing the screen, when 12–14 day old flies were used to allow for time on 30% sucrose/5% yeast food. For these experiments, experimental flies were exposed to donor animals for 48 hours, after which donor flies were removed and experimental flies were assayed. For lifespan experiments, experimental flies were exposed to donor animals beginning on day 2 following eclosion (after sexes had been separated), and exposure continued over the lifetime of the flies.

Lifespan assays

After beginning exposure, lifespan data was collected using *Dlife* computer software[49]. For each lifespan, 100 experimental flies (20 replicate vials containing 5 experimental and 25 donor flies each) were established for all treatment/genotype groups. Flies were transferred

to fresh vials and food every 2–3 days, at which time deaths were recorded. Donor flies were replenished when approximately 75% of donor flies remained (~28 days at 25 °C, ~21 days at 29 °C). Experiments continued until no experimental flies remained alive, at which time donor flies were discarded.

Starvation resistance assays

Following 48 hours of exposure (see "Exposure to donor flies"), experimental flies were placed in fresh vials without donor flies containing 1% agar. For each assay, 50 experimental flies (in vials of 10 flies/vial) were established for all treatment/genotype groups. The number of dead flies in each vial was recorded every 2–4 hours until no experimental flies remained alive.

Fat store (TAG) assays

Following 48 hours of exposure (see "Exposure to donor flies"), experimental flies were quickly frozen in a dry ice bath, then homogenized in 100 μl PBS/0.01% Triton-X in groups of 5 flies per sample, with 5–10 samples per treatment/genotype. Afterward, 5 μl of homogenate was added to 150 μl of Infinity Triglyceride Reagent (Thermo Electron Corp.) and incubated at 37 °C for 10 minutes with constant agitation. Concentrations of triacylglycerides (TAG) were determined by comparing the absorbance at 520 nm of experimental samples to known triglyceride standards.

Neurometabolomic analysis

Following 48 hours of exposure (see "Exposure to donor flies"), experimental flies were quickly frozen in a dry ice bath, and stored at −80 °C overnight. Heads were removed via vortex and separated from body parts by filtering through meshes. Forty to fifty heads were then homogenized for 20 seconds in 200 μl PBS using the Fast Prep 24. Following the addition of 800 μl of methanol, samples were incubated for 30 minutes on dry ice, then homogenized again. The mixture was then spun at 13000 RPM for 5 minutes at 4 °C, and the soluble extract was collected into vials. This extract was then dried using a speedvac at 30 °C for approximately 3 hours. Untargeted global aqueous metabolomics was performed in the Northwest Metabolomics Research Center at the University of Washington using an Agilent 6520 Q-TOF-MS coupled to an Agilent 1200SL UPLC system. This instrument has both ESI and APCI ion sources. Agilent Mass Hunter and Mass Profiler Professional software was used to identify and quantitate metabolites and to analyze metabolite profiles.

Data imputation and PCA analysis

Using untargeted metabolomics, we were able to detect 1463 metabolites for positive mode and 1034 metabolites for negative mode in the first experiment, and 1703 metabolites for positive mode and 1365 metabolites for negative mode in the second experiment. After removing any metabolites missing from more than two samples (60–77%), we were left with 524 and 409 metabolites for positive and negative mode in the first experiment, and 392 and 379 metabolites for positive and negative mode in the second experiment. Metabolite abundance for remaining missing values in this data set were log-transformed and imputed using the k-Nearest Neighbor (KNN) algorithm with the `impute` package of R

Bioconductor (www.bioconductor.org). We then normalized the data to the standard normal distribution (μ=0, σ^2=1). Principal Component Analysis (PCA) was performed using the made4 package of R Bioconductor. We used permutation tests (n=10,000) to select PCs that significantly separate either mating or pheromone effects between different treatments. For each permutation, we randomly distributed the treatments to the real abundance of each metabolite. PC analysis was done for both randomized and real data. The degree of separation for each PC can be measured by analyzing between- and within-group variance based on the projection of samples on that PC, which is indicated by the Z-score:

$$Z = \frac{Variance\ between\ groups}{Variance\ within\ groups},$$

Variance between groups = $\sum_{k=1}^{N} n_k \times (Mean_{total} - Mean_k)^2$, where N indicate the number of groups and n_k indicates the number of samples in Group k. The distribution of Z-score was obtained from 10,000 randomized datasets. PCs that significantly deviated from this randomized distribution were considered as a significant separation of groups. Individual metabolites whose abundances were associated with either mating or pheromone exposure were identified from positive and negative modes and combined for pathway enrichment analysis using MetaboAnalyst 3.0 (http://www.metaboanalyst.ca).

Temperature-dependent neuronal manipulations

For the corazonin manipulation experiments in which temperature was used to activate or inhibit *crz*-expressing neurons in adult flies, fly eggs from experimental and control genotypes were collected and raised in 18 °C, 12h:12h light:dark incubators. This temperature represents the permissive temperature at which no neuronal effects should manifest. Two days post-eclosion, flies were sexed and sorted as described above. Following experimental set-up, flies were placed at 29 °C (the restrictive temperature for which neuronal activation or inhibition is expected) for the remainder of their lifespan.

Quantitative PCR

Following 48 hours of exposure (see “Exposure to donor flies”), experimental flies were quickly frozen in a dry ice bath. RNA was extracted using Trizol (Invitrogen) from 3–5 samples per treatment, with each sample containing 25 experimental flies. cDNA was then synthesized using the Superscript III first strand synthesis kit (Invitrogen). Quantitative real-time PCR was performed with SYBR green from SA Biosciences. Expression was normalized to expression of the housekeeping gene *rp49*. All reactions were performed in duplicate for technical replication. If no exponential amplification was observed, the sample was removed from analysis. The following primers were used:

4EBP Forward: CGAACAGCCAACGGTGAACA

4EBP Reverse: TTCCGCTGGACGTGTAAGCA

RP49 Forward: ACTCAATGGATACTGCCAG

RP49 Reverse: CAAGGTGTCCCACTAATGCAT

Circulating dILP2 ELISA

Following exposure of flies carrying a FLAG-tagged *dIlp2* allele to the indicated donor flies[50] for 48 hours, hemolymph was extracted by skewering flies with a large needle, then immediately spinning them at 5000 × g for 5 minutes at 4 °C in a .6 ml tube perforated at the bottom with a 16-gage needle, placed in a 2 ml tube. The hemolymph was collected from the bottom of the 2ml enclosing tube. ELISA assays were performed as described previously, using flies with FLAG-tagged dILP2[50].

Mating latency assays

To measure the influence of masculinization on female mating latency, we flipped individual Canton-S male flies into vials containing either a single control female (w^{1118};;*UAS-TRA*^{DSRNA}/+), a single masculinized female (w^{1118};*OK72-Gal4*/+;*UAS-TRA*^{DSRNA}/+), or one control female and one masculinized female (i.e. competition vials). The vial plug was located roughly 1 inch from the top of the food to limit space and promote interactions. Vials were monitored at least once every 10–15min, and time to copulation and genotype of the mating female (for competition vials) were recorded when the male was seen to successfully mount the female. Likelihood-ratio tests were used to obtain P-values for the hypothesis of identical rates between treatments. Vials were observed for 6 hours.

Fertilization assays

Fertilization assays were used to quantify *successful* mating rates of males with control and masculinized females. These experiments were performed by adding 1 male ($y^{-}w^{-}$) and 1 female (either wild-type or masculinized) to a vial. Flies were then allowed to interact overnight (12 hours), after which the male was removed. If evidence of larval development was not observed after 1 week, it was assumed no successful fertilization occurred.

Offspring assays

To measure the lifetime offspring production, lifespan experiments were performed as described (above) with the additional requirement that all vials within the assay period were saved and incubated at 25 °C. Offspring were allowed to emerge for two weeks, after which all flies were frozen and counted.

Video Analysis

Eight-day old, mated experimental *yw* male flies were lightly gassed and placed singly into 10 separate vials containing standard fly media and 5 donor flies [control male (w^{1118};*UAS-TRA*/+;+), feminized male (w^{1118};*OK72-Gal4*/*UAS-TRA*;+), control females (w^{1118};+;*UAS-TRA*^{DSRNA}/+), or masculinized females (w^{1118};*OK72-Gal4*/+;*UAS-TRA*^{DSRNA}/+)]. After 24 hours, flies in each vial were mouth pipetted into circular video arenas containing 5% sucrose and 2% agar. The arenas were placed into a 25°C incubator with 12:12 light: dark cycles with color video cameras (placement of each treatment in the incubator was randomized). After 24 hours, we collected 6 hours of video from each treatment. The videos were analyzed over a random 10 minute interval where the total number of interactions (every time the experimental male touches, displays wing courtship song, and/or closely chases a donor fly) and the total interaction time (the total time the

experimental male touches, displays wing courtship song, and/or closely chases a donor fly) were quantified.

Wing Damage Assay

Five 8-day old, mated experiment *yw* males with intact wings were lightly gassed and placed into 10 separate vials containing standard fly media and 25 donor flies [control male (w^{1118};*UAS-TRA*/+;+), feminized male (w^{1118};*OK72-Gal4*/*UAS-TRA*;+), control females (w^{1118};+;$UAS\text{-}TRA^{DSRNA}$/+), or masculinized females (w^{1118};*OK72-Gal4*/+;$UAS\text{-}TRA^{DSRNA}$/+)]. The vials were kept in a 25°C incubator with 12:12 light: dark cycles for 2 weeks; fresh food was given every Monday, Wednesday, and Friday during this exposure period. The flies were then anesthetized and the wing condition of each experimental male was assessed in a double blind fashion according to the following scale: 0 = males with no wing damage, 1 = males with >10% wing damage, 2 = males with 10–50% wing damage, and 3 = males with ≥50% wing damage.

Statistics

Unless otherwise indicated, group- and pairwise-comparisons among survivorship curves (both lifespan and starvation) were performed using the DLife computer software[49] and the statistical software R. P-values were obtained using Cox-regression tests (select pairwise comparisons and group comparisons or interaction studies) as noted. For all box plots, box represents Standard Error of the Mean (SEM, centered on the mean), whiskers represent 10%/90%, and the horizontal line represents the median.

Data availability

Metabolomics data and analyses are provided as Supplementary File 1. All additional data are available upon request from the corresponding author.

Supplementary Material

Refer to Web version on PubMed Central for supplementary material.

Acknowledgments

Members of the Pletcher laboratory provided comments on the experimental design and analysis. This research was supported by US National Institutes of Health (R01AG030593 and R01AG051649 to S.D.P., R01AG049494 to D.E.L.P., and R01GM102279 to S.D.P and D.E.L.P.), the Glenn Medical Foundation (to S.D.P.) a Ruth L. Kirschstein National Research Service Award from NIA (F30AG048661, to Z.M.H.), and the University of Michigan Systems Biology Training Grant (T32GM008322, to Z.M.H.).

References

1. Reznick D. Measuring the costs of reproduction. Trends in ecology & evolution. 1992; 7:42–45. DOI: 10.1016/0169-5347(92)90104-J [PubMed: 21235948]
2. Browne RA. The Costs of Reproduction in Brine Shrimp. Ecology. 1982; 63:43–47. DOI: 10.2307/1937029
3. Van Voorhies WA. Production of sperm reduces nematode lifespan. Nature. 1992; 360:456–458. DOI: 10.1038/360456a0 [PubMed: 1448167]
4. Maynard Smith J. The Effects of Temperature and of Egg-Laying on the Longevity of Drosophila-Subobscura. J Exp Biol. 1958; 35:832–842.

5. Koivula M, Koskela E, Mappes T, Oksanen TA. Cost of reproduction in the wild: Manipulation of reproductive effort in the bank vole. Ecology. 2003; 84:398–405. DOI: 10.1890/0012-9658(2003)084[0398:Coritw]2.0.Co;2
6. Hoffman CL, et al. Sex differences in survival costs of reproduction in a promiscuous primate. Behav Ecol Sociobiol. 2008; 62:1711–1718. DOI: 10.1007/s00265-008-0599-z [PubMed: 23645968]
7. Dallerac R, et al. A delta 9 desaturase gene with a different substrate specificity is responsible for the cuticular diene hydrocarbon polymorphism in Drosophila melanogaster. Proc Natl Acad Sci U S A. 2000; 97:9449–9454. doi: 10.1073/pnas.150243997.150243997 [pii]. [PubMed: 10920187]
8. Min KJ, Lee CK, Park HN. The lifespan of Korean eunuchs. Curr Biol. 2012; 22:R792–R793. [PubMed: 23017989]
9. Stearns, SC. The Evolution of Life Histories. Oxford University Press; 1992.
10. Speakman JR. The physiological costs of reproduction in small mammals. Philosophical transactions of the Royal Society of London Series B, Biological sciences. 2008; 363:375–398. DOI: 10.1098/rstb.2007.2145 [PubMed: 17686735]
11. Harshman LG, Zera AJ. The cost of reproduction: the devil in the details. Trends in ecology & evolution. 2007; 22:80–86. DOI: 10.1016/j.tree.2006.10.008 [PubMed: 17056152]
12. Flatt T. Survival costs of reproduction in Drosophila. Exp Gerontol. 2011; 46:369–375. doi: 10.1016/j.exger.2010.10.008S0531-5565(10)00354-2[pii]. [PubMed: 20970491]
13. Salmon AB, Marx DB, Harshman LG. A cost of reproduction in Drosophila melanogaster: stress susceptibility. Evolution. 2001; 55:1600–1608. [PubMed: 11580019]
14. Chapman T, Hutchings J, Partridge L. No Reduction in the Cost of Mating for Drosophila-Melanogaster Females Mating with Spermless Males. P Roy Soc B-Biol Sci. 1993; 253:211–217. DOI: 10.1098/rspb.1993.0105
15. Zajitschek F, Zajitschek SR, Friberg U, Maklakov AA. Interactive effects of sex, social environment, dietary restriction, and methionine on survival and reproduction in fruit flies. Age (Dordr). 2013; 35:1193–1204. DOI: 10.1007/s11357-012-9445-3 [PubMed: 22798158]
16. Wigby S, Chapman T. Sex peptide causes mating costs in female Drosophila melanogaster. Curr Biol. 2005; 15:316–321. DOI: 10.1016/j.cub.2005.01.051 [PubMed: 15723791]
17. Cordts R, Partridge L. Courtship reduces longevity of male Drosophila melanogaster. Anim Behav. 1996; 52:269–278. DOI: 10.1006/anbe.1996.0172
18. O'Brien DM, Min KJ, Larsen T, Tatar M. Use of stable isotopes to examine how dietary restriction extends Drosophila lifespan. Curr Biol. 2008; 18:R155–156. doi: 10.1016/j.cub.2008.01.021S0960-9822(08)00067-5[pii]. [PubMed: 18302914]
19. Djawdan M, Sugiyama TT, Schlaeger LK, Bradley TJ, Rose MR. Metabolic Aspects of the Trade-Off between Fecundity and Longevity in Drosophila melanogaster. Physiological Zoology. 1996; 69:1176–1195. DOI: 10.1086/physzool.69.5.30164252
20. Barnes AI, Wigby S, Boone JM, Partridge L, Chapman T. Feeding, fecundity and lifespan in female Drosophila melanogaster. Proceedings Biological sciences/The Royal Society. 2008; 275:1675–1683. DOI: 10.1098/rspb.2008.0139
21. Sujkowski A, Bazzell B, Carpenter K, Arking R, Wessells RJ. Endurance exercise and selective breeding for longevity extend Drosophila healthspan by overlapping mechanisms. Aging (Albany NY). 2015; 7:535–552. [PubMed: 26298685]
22. Maures TJ, et al. Males shorten the life span of C. elegans hermaphrodites via secreted compounds. Science. 2014; 343:541–544. DOI: 10.1126/science.1244160 [PubMed: 24292626]
23. Gendron CM, et al. Drosophila life span and physiology are modulated by sexual perception and reward. Science. 2014; 343:544–548. DOI: 10.1126/science.1243339 [PubMed: 24292624]
24. Shi C, Murphy CT. Mating induces shrinking and death in Caenorhabditis mothers. Science. 2014; 343:536–540. DOI: 10.1126/science.1242958 [PubMed: 24356112]
25. Thistle R, Cameron P, Ghorayshi A, Dennison L, Scott K. Contact Chemoreceptors Mediate Male-Male Repulsion and Male-Female Attraction during Drosophila Courtship. Cell. 2012; 149:1140–1151. DOI: 10.1016/j.cell.2012.03.045 [PubMed: 22632976]
26. Shohat-Ophir G, Kaun KR, Azanchi R, Heberlein U. Sexual deprivation increases ethanol intake in Drosophila. Science. 2012; 335:1351–1355. DOI: 10.1126/science.1215932 [PubMed: 22422983]

27. Wu Q, Zhao Z, Shen P. Regulation of aversion to noxious food by Drosophila neuropeptide Y- and insulin-like systems. Nature neuroscience. 2005; 8:1350–1355. DOI: 10.1038/nn1540 [PubMed: 16172603]
28. Junger MA, et al. The Drosophila forkhead transcription factor FOXO mediates the reduction in cell number associated with reduced insulin signaling. J Biol. 2003; 2:20. [PubMed: 12908874]
29. Rera M, Clark RI, Walker DW. Intestinal barrier dysfunction links metabolic and inflammatory markers of aging to death in Drosophila. Proc Natl Acad Sci U S A. 2012; 109:21528–21533. doi: 10.1073/pnas.1215849110 1215849110 [pii]. [PubMed: 23236133]
30. Landis G, Shen J, Tower J. Gene expression changes in response to aging compared to heat stress, oxidative stress and ionizing radiation in Drosophila melanogaster. Aging (Albany NY). 2012; 4:768–789. [PubMed: 23211361]
31. Slack C, Giannakou ME, Foley A, Goss M, Partridge L. dFOXO-independent effects of reduced insulin-like signaling in Drosophila. Aging cell. 2011; 10:735–748. DOI: 10.1111/j.1474-9726.2011.00707.x [PubMed: 21443682]
32. Weber K, Johnson N, Champlin D, Patty A. Many P-element insertions affect wing shape in Drosophila melanogaster. Genetics. 2005; 169:1461–1475. [PubMed: 15545659]
33. Broughton SJ, et al. DILP-producing median neurosecretory cells in the Drosophila brain mediate the response of lifespan to nutrition. Aging cell. 2010; 9:336–346. DOI: 10.1111/j.1474-9726.2010.00558.x [PubMed: 20156206]
34. Gronke S, Clarke DF, Broughton S, Andrews TD, Partridge L. Molecular evolution and functional characterization of Drosophila insulin-like peptides. PLoS genetics. 2010; 6:e1000857. [PubMed: 20195512]
35. Hwangbo DS, Gershman B, Tu MP, Palmer M, Tatar M. Drosophila dFOXO controls lifespan and regulates insulin signalling in brain and fat body. Nature. 2004; 429:562–566. [PubMed: 15175753]
36. Lu B, LaMora A, Sun Y, Welsh MJ, Ben-Shahar Y. ppk23-Dependent chemosensory functions contribute to courtship behavior in Drosophila melanogaster. PLoS genetics. 2012; 8:e1002587. [PubMed: 22438833]
37. Wen T, Parrish CA, Xu D, Wu Q, Shen P. Drosophila neuropeptide F and its receptor, NPFR1, define a signaling pathway that acutely modulates alcohol sensitivity. Proc Natl Acad Sci U S A. 2005; 102:2141–2146. doi: 0406814102 [pii] 10.1073/pnas.0406814102. [PubMed: 15677721]
38. Fowler K, Partridge L. A cost of mating in female fruitflies. Nature. 1989; 338:760–761.
39. Soma KK, Francis RC, Wingfield JC, Fernald RD. Androgen regulation of hypothalamic neurons containing gonadotropin-releasing hormone in a cichlid fish: integration with social cues. Hormones and behavior. 1996; 30:216–226. DOI: 10.1006/hbeh.1996.0026 [PubMed: 8918677]
40. Zhang G, et al. Hypothalamic programming of systemic ageing involving IKK-beta, NF-kappaB and GnRH. Nature. 2013; 497:211–216. DOI: 10.1038/nature12143 [PubMed: 23636330]
41. Gaikwad A, Biju KC, Muthal PL, Saha S, Subhedar N. Role of neuropeptide Y in the regulation of gonadotropin releasing hormone system in the forebrain of Clarias batrachus (Linn.): immunocytochemistry and high performance liquid chromatography-electrospray ionization-mass spectrometric analysis. Neuroscience. 2005; 133:267–279. DOI: 10.1016/j.neuroscience.2004.12.052 [PubMed: 15893649]
42. Turi GF, Liposits Z, Moenter SM, Fekete C, Hrabovszky E. Origin of neuropeptide Y-containing afferents to gonadotropin-releasing hormone neurons in male mice. Endocrinology. 2003; 144:4967–4974. DOI: 10.1210/en.2003-0470 [PubMed: 12960087]
43. Anderson DJ, Adolphs R. A framework for studying emotions across species. Cell. 2014; 157:187–200. DOI: 10.1016/j.cell.2014.03.003 [PubMed: 24679535]
44. Kato K, Zweig R, Schechter CB, Barzilai N, Atzmon G. Positive attitude toward life, emotional expression, self-rated health, and depressive symptoms among centenarians and near-centenarians. Aging Ment Health. 2016; 20:930–939. DOI: 10.1080/13607863.2015.1056770 [PubMed: 26114814]
45. Lindau ST, et al. A study of sexuality and health among older adults in the United States. N Engl J Med. 2007; 357:762–774. doi: 357/8/762[pii] 10.1056/NEJMoa067423. [PubMed: 17715410]

46. Brody S. Blood pressure reactivity to stress is better for people who recently had penile-vaginal intercourse than for people who had other or no sexual activity. Biol Psychol. 2006; 71:214–222. doi: S0301-0511(05)00073-6[pii] 10.1016/j.biopsycho.2005.03.005. [PubMed: 15961213]

47. Lewis E. A new standard food medium. Drosophila Information Service. 1960; 34:117–118.

48. Kondo S, Ueda R. Highly improved gene targeting by germline-specific Cas9 expression in Drosophila. Genetics. 2013; 195:715–721. DOI: 10.1534/genetics.113.156737 [PubMed: 24002648]

49. Linford NJ, Bilgir C, Ro J, Pletcher SD. Measurement of Lifespan in Drosophila melanogaster. Jove-J Vis Exp. 2013 doi: UNSPe 50068 10.3791/50068.

50. Pasco MY, Leopold P. High sugar-induced insulin resistance in Drosophila relies on the lipocalin Neural Lazarillo. PLoS One. 2012; 7:e36583. doi: 10.1371/journal.pone.0036583PONE-D-12-00807[pii]. [PubMed: 22567167]

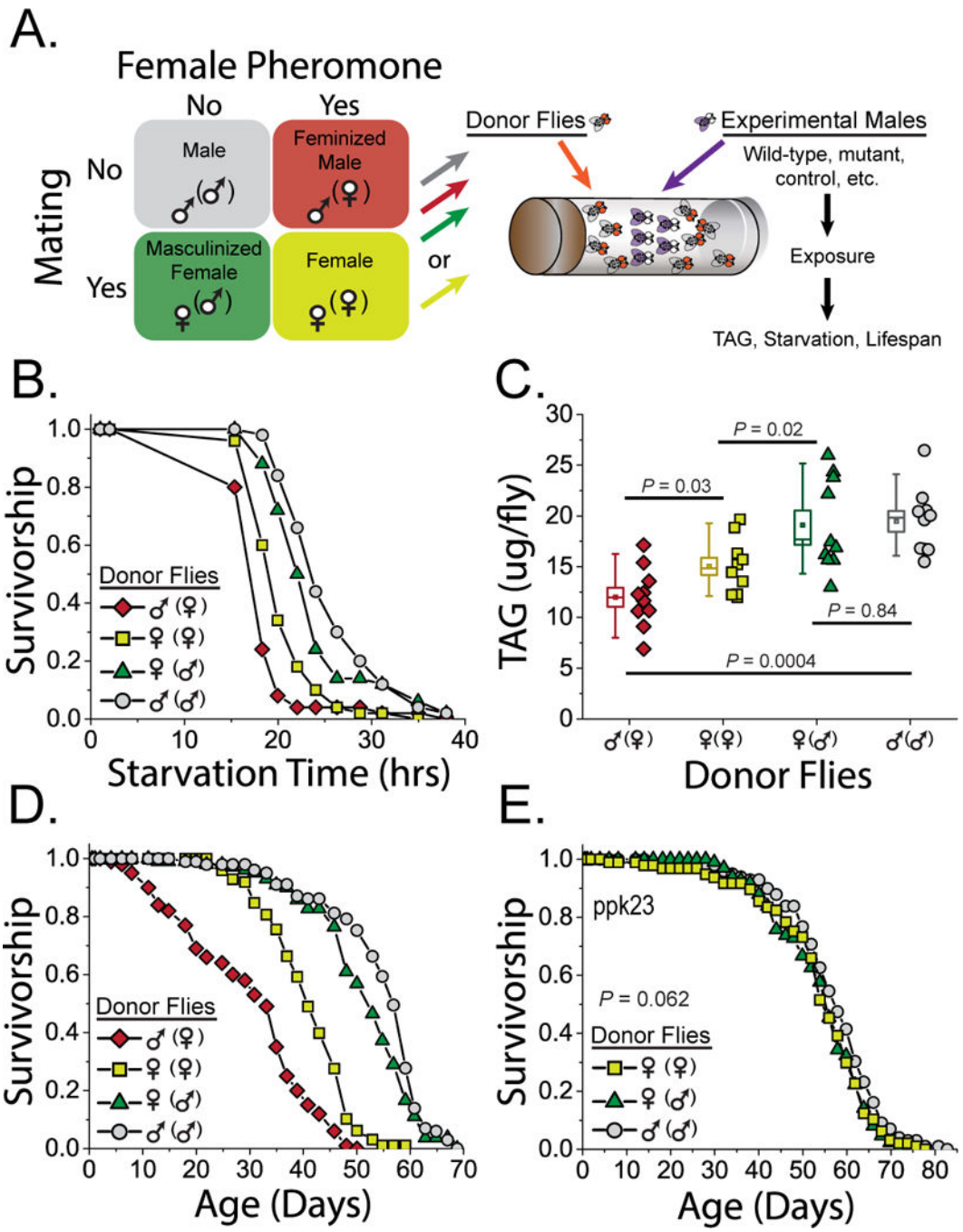

Figure 1. Pheromone exposure, and not mating, drives the physiologic costs of reproduction

(A) Experimental design used to distinguish effects of pheromone perception from effects of mating. (B) The presence of female pheromones reduced male starvation resistance both in presence of mating (compare yellow and green lines, P = 0.00028) and in the absence of mating (compare grey and red lines, P < 0.00001). Mating was beneficial in the context of female pheromone perception (compare red and yellow lines, P = 0.0022) but had no effect in their absence (compare green and grey lines, P = 0.16). N = 50 flies per group. (C) A similar pattern was observed for (C) triacylglyceride (TAG) storage (n = 10 biological

replicates of 5 flies each per group) and (D) lifespan (N = 100 flies per group). Pairwise P-values were determined by two-tailed t-test (TAG abundance). Pairwise comparisons of survival curves are as follow: yellow vs. green lines, $P < 0.00001$; grey vs. red lines, $P < 0.00001$; yellow vs. red lines, $P < 0.00001$; green vs. grey lines, $P = 0.020$. (E) The lifespan of *ppk23* mutant males, which cannot perceive pheromones, was statistically indistinguishable regardless of the presence of mating ($P = 0.076$ comparing grey and yellow lines) or pheromones ($P = 0.72$, compare yellow and green lines). N = 100 flies per group. P-values related to survivorship were obtained from Cox regression. In Panel C, the box represents SEM (Standard Error of the Mean, centered on the mean), whiskers represent 10%/90%, and the horizontal line represents the median.

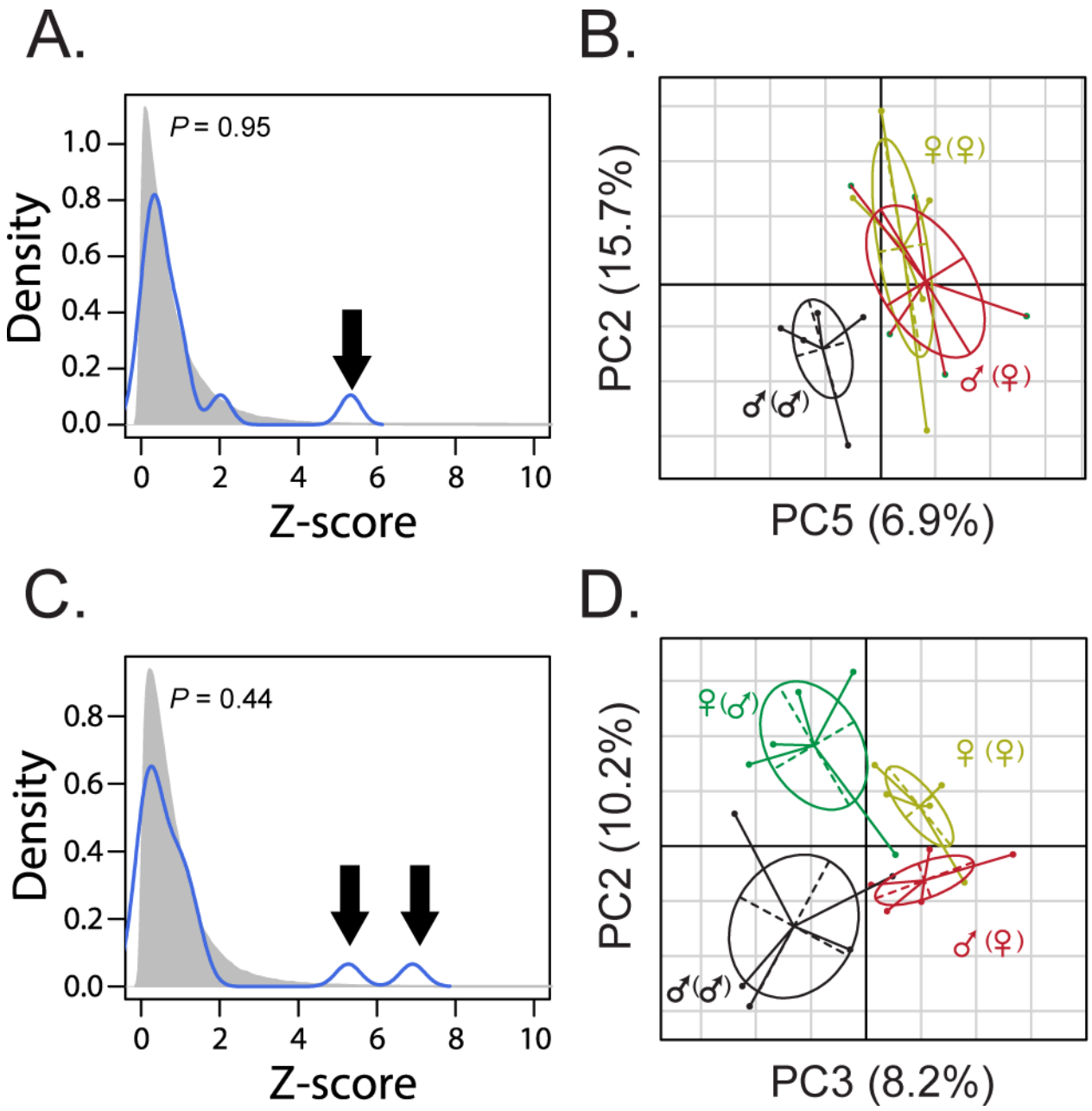

Figure 2. Pheromone exposure and mating drive separate, global changes in the neurometabolome

(A) Observed (blue) and randomized (grey) distributions of the ability of individual principal components to effectively distinguish neurometabolomic signatures of experimental males. No statistical difference was observed between these two distributions (P = 0.95, Kolmogorov-Smirnov Test). This analysis identified a single PC, PC5, that provides significant separation between groups of experimental males (P = 0.017, permutation test, see Methods). (B) PC plot showing the distribution of samples for each treatment. N = 5 biological replicates of 40 – 50 fly heads per group. (C) Observed (blue) and randomized (grey) distributions of the ability of individual principal components to effectively distinguish neurometabolomic signatures of experimental males. No statistical difference

was observed between these two distributions (P = 0.44, Kolmogorov-Smirnov Test). This analysis, which included animals exposed to all four types of donor flies, identified two PCs (PC2 and PC3) that exhibited statistically significant ability to distinguish exposure groups (P = 0.0018 for PC2, P = 0.0056 for PC3, permutation test, see Methods). (D) PC plot showing the distribution of samples for each treatment. Neurometabolites in PC2 separate exposures based on mating status, whereas neurometabolites in PC3 separate exposures based on pheromone perception. Analyses represent mass spec analysis of metabolites identified under positive mode. N = 5 biological replicates of 40 – 50 fly heads per group.

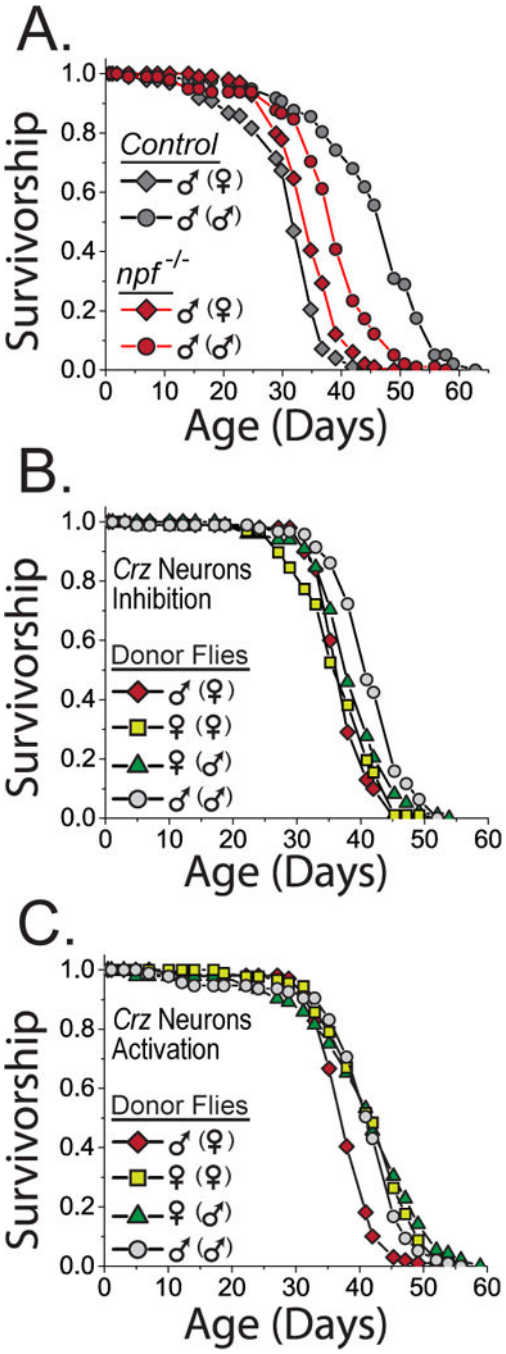

Figure 3. Self-imposed costs of reproduction are mediated by specific peptidergic neurons

(A) A mutation in the neuropeptide gene *npf* suppressed ($P < 0.00001$ interaction term in Cox regression), but did not eliminate ($P < 0.00001$ examining the effect of feminized male exposure in $npf^{-/-}$ males) the effect of pheromone exposure on lifespan. (B) Spatiotemporal inhibition of *crz*-expressing neurons in adult male flies using a combination of a temperature-sensitive *Gal80* and the potassium rectifying channel $Kir^{2.1}$ (*UAS-kir2.1*;*tub5-Gal80*^{ts} x *crz-Gal4*) eliminated the beneficial effects of mating in the presence of female pheromones ($P = 0.48$, comparing feminized male and control female groups). (C)

Spatiotemporal activation of *crz*-expressing neurons (*UAS-TrpA1 x crz-Gal4*) potentiated the beneficial effects of mating such that the reduction of lifespan caused by pheromone exposure was completely reversed by allowing mating ($P = 0.31$ comparing exposure to control females to control males). In both panels (B) and (C), exposure to feminized males significantly decreases lifespan compared to wild-type male exposure ($P < 0.00001$). When compared to the control lifespan in Figure S6, exposure to wild-type males leads to no differences (for each of the three comparisons, $P > 0.86$). However, exposure to wild-type females leads to a decrease in lifespan upon inhibition ($P = 0.0044$ compared to control) and an increase in lifespan upon activation ($P = 0.0047$ compared to control). Lifespans are shorter, and exposure effects are compressed, in these experiments, which were conducted at a high temperature for neuronal manipulations (29°C). For all experiments in this figure, $N = 100$ flies per group.

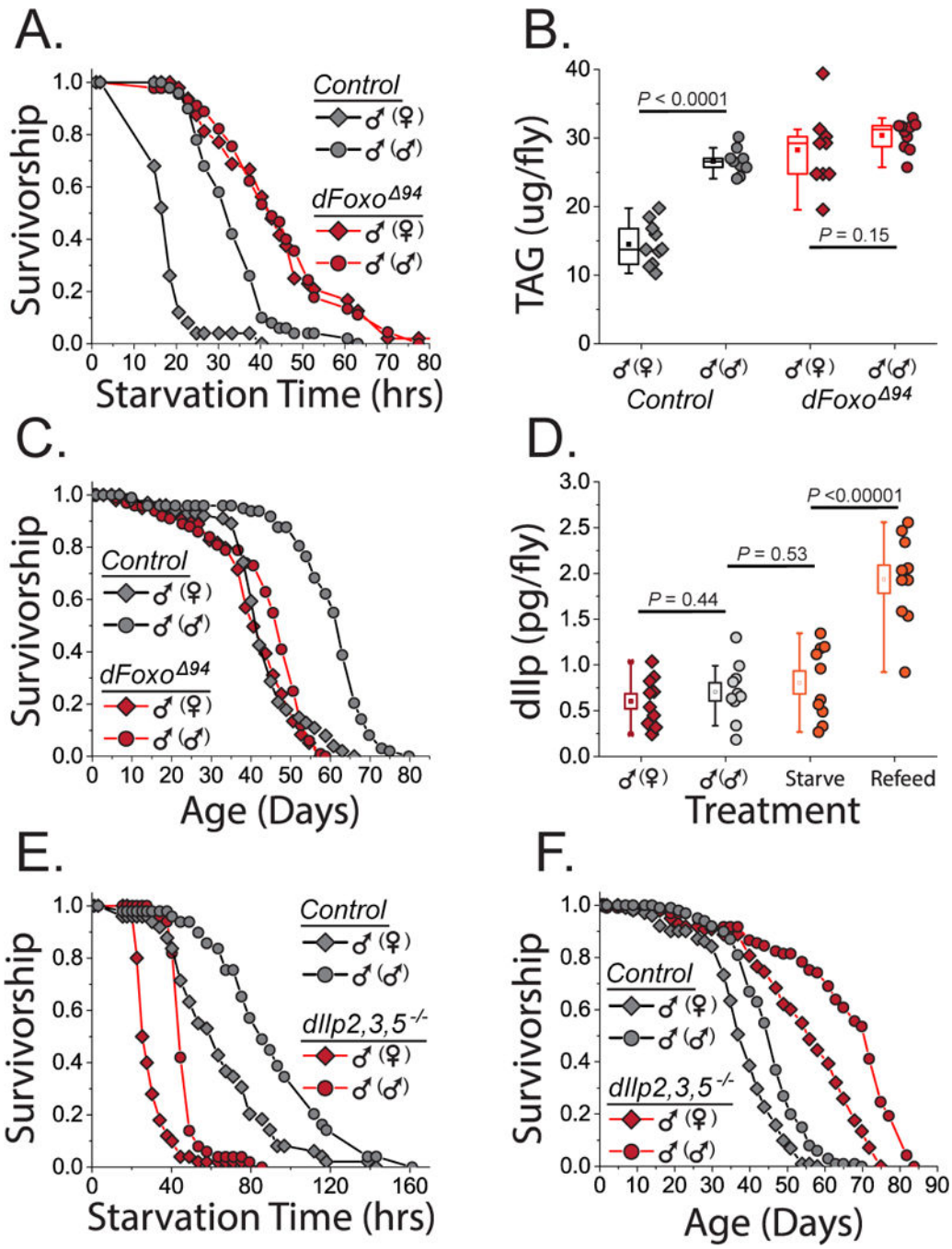

Figure 4. Self-imposed costs of reproduction are mediated through *dFoxo* signaling by a dILP2/3/5 independent mechanism

Male flies carrying loss of function alleles for the transcription factor *dFoxo* (*dFoxo*$^{\Delta 94}$) were resistant to the effects of pheromones on (A) starvation resistance (P = 0.90, control responds as expected P < 0.00001, N = 50 flies per group), (B) fat stores (P values from one-tailed t-test, N = 10 biological replicates for control ♂(♀) and *dFoxo* ♂(♂), N = 9 biological replicates for control ♂(♂) and *dFoxo* ♂(♀), each composed of 5 flies), and (C) lifespan, where mutant males retained a minimal but significant longevity response (P = 0.018,

control responds as expected $P < 0.00001$, N = 100 flies per group). (D) Circulating dILP2 levels were not significantly affected by exposure to feminized males. Starvation and refeeding after starvation were used as negative and positive controls, respectively. N = 10 biological replicates composed of the hemolymph of 20 flies each. (E) The starvation resistance of males carrying deletions of three dIlps expressed in the insulin-producing cells in the *pars intercerebralis* (*dILP2,dILP3,dILP5*) responded strongly to pheromone exposure ($P < 0.00001$), similar to animals of a control genetic background (w^{dah}; $P = 0.00010$). N = 50 flies per group. (F) Males mutant for *dILP2,dILP3,dILP5* also demonstrate decreased longevity in response to pheromone exposure ($P < 0.00001$), similar to animals of a control genetic background (w^{dah}; $P < 0.00001$), suggesting that pheromones alter aging through a dILP2/3/5-independent pathway. N = 100 flies per group. In panels B and D, the box represents SEM, whiskers represent 10%/90%, and the horizontal line represents the median.